J. Fluid Mech. (1979), *vol.* 93, *part* 2, *pp.* 241–250
Printed in Great Britain

Time similarity analysis of unsteady buoyant plumes in neutral surroundings

By M. A. DELICHATSIOS

Factory Mutual Research, 1151 Boston-Providence Turnpike, Norwood, Massachusetts 02062

(Received 16 February 1978 and in revised form 31 July 1978)

A time similarity formulation of the flow equations for unsteady plumes is shown to exist only when the buoyancy flux at the source varies as a power function of time. The time similarity equations for unsteady plumes are solved numerically. It is shown that the velocity of the leading edge of the plume is less (at most the 0·42 fraction) than the velocity inside the plume behind its leading edge; this observation is consistent with Turner's (1962) results on the behaviour of a starting plume with constant buoyancy flux at the source. Finally, experimental results of axial temperature histories in the buoyant plume generated by a fast-growing fire are compared with the theoretical predictions.

1. Introduction

Buoyant plumes originating from growing fires are unsteady; i.e. the buoyancy flux varies with time. Knowledge of the temperature histories in unsteady plumes is required to predict, for example, the response of detectors in fast-growing fires. The present study is a continuation of the work of Heskestad (1972), who developed functional correlations of temperature histories in unsteady plumes, based on dimensional arguments.

The development of the present work is based on an extension of Turner's (1962) model of the flow field associated with a starting plume of constant buoyancy flux at the source. The flow generated by an unsteady plume is visualized as consisting of the flow inside the plume and the flow in the front preceding the plume. The advancing front may be modelled as a spherical thermal. The front attached to the plume advances through stationary fluid, where it becomes mixed with its surroundings, while at the same time additional fluid drawn up into the advancing front from the plume imparts to it extra buoyancy and momentum.

Only the flow properties inside the unsteady plume are derived in this work. In §2 the time similarity formulation of the integral unsteady plume equations is developed. It is shown that a time similarity formulation exists only when the buoyancy flux at the source varies as a power function of time. In §3 a renormalization and the numerical solution of the unsteady plume equations is presented, together with one asymptotic solution. It is also shown that the velocity at the leading edge of the plume (which is defined here to coincide with the base of the thermal) is less (at most the 0·42 fraction) than the velocity inside the plume behind the leading edge. Finally, in §4 the theoretical results are compared with experimental temperature histories inside the plume generated by a fast-growing fire.

0022–1120/79/4252–7030 $02.00

2. Unsteady plume equations and similarity analysis

An unsteady plume is preceded by a thermal cap, in the same manner as a developing plume of constant buoyancy flux [see, e.g., Turner (1962) and Middleton (1975)]. The base of the thermal cap is defined also as the leading edge of the plume.

The unsteady plume equations are derived assuming the usual weak plume approximations (Middleton 1975) with Gaussian profiles (Morton 1959) for the mean velocity and mean buoyancy flux. Cylindrical co-ordinates (r, z) with z upwards are used. The time is represented by t.

Consistent with the above assumptions, the integral equations for mass, momentum and energy conservation in an unsteady plume are

$$\frac{\partial r_0^2}{\partial t}+\frac{\partial}{\partial z}(r_0^2 U) = 2ar_0 U, \tag{2.1}$$

$$\frac{\partial(r_0^2 U)}{\partial t}+\frac{1}{2}\frac{\partial}{\partial z}(r_0^2 U^2) = \lambda^2 r_0^2 B, \tag{2.2}$$

$$\frac{\partial}{\partial t}(r_0^2 B)+\frac{1}{1+\lambda^2}\frac{\partial}{\partial z}(r_0^2 UB) = 0, \tag{2.3}$$

where a is the entrainment coefficient, assumed constant; $r_0(z, t)$ represents the momentum lateral spread; $\lambda r_0(t, z)$ represents the lateral spread of heat; and $U(z, t)$ and $B(z, t)$ are the axial values of the mean velocity and mean buoyancy, respectively.

For a virtual point source of buoyancy, the mass flux, momentum flux and buoyancy flux are zero at the beginning ($t = 0$) of buoyancy flux release (initial conditions). The buoyancy flux at the source, $F(t)$, is related to the plume properties by

$$(r_0^2 UB)(z = 0, t) = \frac{\lambda^2+1}{\lambda^2\pi}F(t), \tag{2.4}$$

while the mass flux and momentum flux at the source are zero at all times (boundary conditions).

In a time similarity formulation the appropriate velocity scale is the velocity at the base of the thermal cap (leading edge of plume) $U_{LE}(t)$ and the appropriate length scale is the distance of the leading edge from the virtual source $z_{LE}(t)$. To be consistent with time similarity theories (e.g. Hansen 1967) the dimensionless variables should be

$$\tilde{r} = \frac{r_0}{z_{LE}(t)}, \tag{2.5}$$

$$\tilde{U} = \frac{U}{\Phi_{LE}(t)}, \tag{2.6}$$

$$\tilde{B} = \frac{B}{d/dt\, U_{LE}(t)}, \tag{2.7}$$

$$\tilde{z} = \frac{z}{z_{LE}(t)}, \tag{2.8}$$

$(\tilde{r}, \tilde{U}, \tilde{B})$ being functions of $\tilde{z}$ and t. The independent variable $\tilde{z}$ indicates physically the relative vertical location of a point inside the plume with respect to the location of the leading edge and assumes values from 0 to 1.

A similarity formulation would be possible if all the dimensionless variables ($\tilde{r}$, $\tilde{U}$, $\tilde{B}$) are explicit functions of only the dimensionless vertical distance ($\tilde{z}$) and implicitly dependent on time through $\tilde{z}$. By writing the unsteady plume equations and the associated initial and boundary conditions in terms of dimensionless variables [(2.5), (2.6), (2.7) and (2.8)], it is found that the necessary condition for a time similarity formulation to exist is

$$Z_{LE}(t) = At^n, \tag{2.9}$$

and

$$(\tilde{r}^2\tilde{U}\tilde{B})\,A^4t^{4n-3}n^2(n-1) = \frac{\lambda^2+1}{\lambda^2\pi}F(t) \quad \text{at} \quad \tilde{z}=0, \tag{2.10}$$

where A and n are constants. From (2.10), which has been derived from (2.4), we can conclude that similarity solutions would exist only if the buoyancy flux $F(t)$ is a power law function of time,

$$F(t) = ft^p. \tag{2.11}$$

It follows from (2.10) that

$$n = \tfrac{1}{4}(p+3), \tag{2.12a}$$

and

$$(\tilde{r}^2\tilde{U}\tilde{B})\,(\text{at } \tilde{z}=0) = \frac{(\lambda^2+1)f}{\lambda^2A^4n^2(n-1)}. \tag{2.12b}$$

The constant A remains undetermined ; physically, it defines the location of the leading edge [cf. (2.9)]; it could be determined either experinentally or by coupling the motion of the plume with the motion of the thermal cap preceding the plume.

3. Renormalization and numerical solutions of the similarity equations

The unsteady plume equations expressed in terms of the dimensionless variables [(2.5), (2.6), (2.7) and (2.8)] accept an asymptotic solution for $\tilde{z}\to 0$:

$$\tilde{r}_0 = \tfrac{6}{5}a\tilde{z}, \tag{3.1a}$$

$$\tilde{U}_0 = \frac{a_1}{n}\tilde{z}^{-\frac{1}{3}}, \tag{3.1b}$$

$$\tilde{B}_0 = \frac{2a_1^2}{3n(n-1)\lambda^2}\tilde{z}^{-\frac{5}{3}}, \tag{3.1c}$$

where

$$a_1 = \left(\frac{25}{24}\frac{c}{a^2}\right)^{\frac{1}{3}}, \tag{3.1d}$$

with

$$c = \frac{(\lambda^2+1)f}{\pi A^4}. \tag{3.1e}$$

It can be shown that the previous solution reduces in terms of physical variables to the so-called quasi-steady approximation. In the quasi-steady approximation the properties of the plume are obtained from the steady plume solutions with the buoyancy flux equal to its instantaneous value (Heskestad 1972).

Normalized variables are introduced using the above asymptotic solution:

$$\bar{r} = \frac{\tilde{r}}{\tilde{r}_0}, \tag{3.2a}$$

$$\bar{U} = \frac{\tilde{U}}{\tilde{U}_0}, \tag{3.2b}$$

$$\bar{B} = \frac{\tilde{B}}{\tilde{B}_0}. \tag{3.2c}$$

The normalized variables express physically the ratio of the unsteady plume properties to the corresponding quasi-steady values.

It has been found by inspection that the following independent variable facilitates the numerical calculations:

$$\bar{z} = \frac{p\tilde{z}^{\frac{4}{3}}}{a_1}. \tag{3.3}$$

The independent variable $\bar{z}$ takes on values from 0 to p/a_1.

In terms of the normalized variables, the flow equations (2.1), (2.2) and (2.3) take the form

$$8\bar{z}\frac{d\bar{r}}{d\bar{z}}\left(\frac{n}{p}\bar{z} - \bar{U}\right) = 5\bar{U}(\bar{r}-1) + 4\bar{r}\bar{z}\frac{d\bar{U}}{d\bar{z}}. \tag{3.4a}$$

$$4\frac{n}{p}\bar{z}^2\frac{d\bar{U}}{d\bar{z}} = \bar{U}\bar{z} - 2\bar{B} + 5\frac{\bar{U}^2}{\bar{r}} - 3\bar{U}^2 - 4\frac{\bar{U}^2}{\bar{r}}\bar{z}\frac{d\bar{r}}{d\bar{z}}, \tag{3.4b}$$

$$\frac{1}{\bar{B}}\frac{d\bar{B}}{d\bar{z}} = \frac{1 + \dfrac{2}{1+\lambda^2}\dfrac{d\bar{U}}{d\bar{z}}}{2\left(\dfrac{n}{p}\bar{z} - \dfrac{\bar{U}}{1+\lambda^2}\right)} - \frac{2}{\bar{r}}\frac{d\bar{r}}{d\bar{z}}, \tag{3.4c}$$

with the following boundary conditions:

$$\left.\begin{aligned}\bar{r} &= 1\\ \bar{U} &= 1\\ \bar{B} &= 1\end{aligned}\right\} \quad \text{at} \quad \bar{z} = 0. \tag{3.5}$$

The system of equations (3.4*a*), (3.4*b*) and (3.4*c*), together with the boundary condition (3.5), has been solved numerically by the simple Euler method. Although it is known that the independent variable $\bar{z}$ varies from 0 to p/a_1, its upper limit is not defined *a priori*. The upper limit determines the position of the leading edge in terms of the variable $\bar{z}$. Its value depends on the value of the unknown factor A [cf. discussion after (2.12*b*)] which determines the position of the leading edge in physical co-ordinates [cf. (2.9)]. We attempted to solve (3.4*a*), (3.4*b*) and (3.4*c*) for all positive values of $\bar{z}$. However, a singularity is observed at the position

$$\frac{n}{p}\bar{z} - \frac{\bar{U}}{1+\lambda^2} = 0. \tag{3.6}$$

It can be shown that, when (3.6) is satisfied, the derivative of the normalized buoyancy $\bar{B}$ cannot be finite. This means that a discontinuity (shock) of buoyancy is to be expected. In other words, (3.6) would give the furthest possible position of the leading edge of the plume without discontinuity in buoyancy. For this location of the leading edge, the velocity inside the plume behind the leading edge (U_1) is related to the leading edge velocity by

$$\frac{U_{LE}}{U_1} = \frac{1}{1+\lambda^2}, \tag{3.7}$$

which is derived from (3.6) and the definitions of $\bar{z}$ (at $Z = Z_{LE}(t)$) and $\bar{U}$ [see (3.2) and (2.5), (2.6), (2.7)]. For locations of the leading edge closer to the origin than the location specified by (3.6), the ratio of the leading edge velocity to the velocity in the plume behind the leading edge can be shown to be less than the value in (3.7).

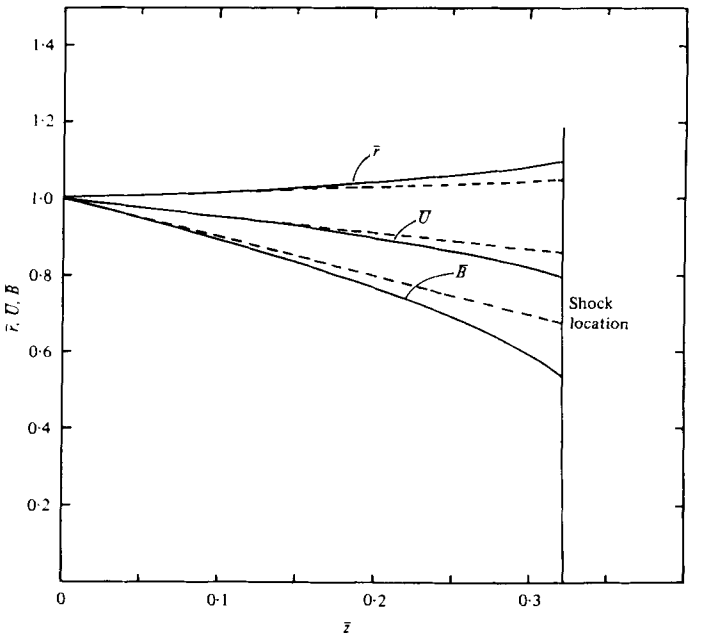

FIGURE 1. Dimensionless radial spread, velocity, and buoyancy of an unsteady plume, expressed as fractions of the quasi-steady values versus the dimensionless vertical position [see (3.9)]. ——, numerical solution; ----, asymptotic approximation [(3.8)], $\lambda = 1{\cdot}16$; $p = 1{\cdot}0$.

Equation (3.7) gives exactly the shock velocity obtained by applying the shock (jump) conditions (see, e.g. Witham 1965) in the initial buoyancy conservation (2.3), with the value of buoyancy after the shock equal to 0 (surrounding conditions). In practical situations no shock will be developed because of the existence of the thermal preceding the plume where the flow conditions do not impose a sudden discontinuity in buoyancy. It follows that the leading edge will be located closer to the origin than (3.6) specifies and that the ratio of the leading edge velocity (at the base of the thermal) to the plume velocity at the same level will be always less than the value given by (3.7). The coefficient at the right-hand side of (3.7) takes on the value 0·42 for the observed value of $\lambda = 1{\cdot}16$ (Middleton 1975). It is important to note that Turner (1962), in his work on the development of a starting plume, obtained a measured value of 0·38 for the velocity coefficient in (3.7). This measured value is less than the maximum theoretical value (0·42), which is consistent with the preceding observation regarding the development of a shock in the buoyancy profile.

The results from the numerical solution are presented now. The numerical solutions are applicable for points inside the plume up to the location of the leading edge. Since the location of the leading edge is not known, the results of the solution of the plume equations are evaluated for the dimensionless variable $\bar{z}$ varying from 0 up to the value specified by (3.6), which determines the maximum possible location of the leading edge before a buoyancy discontinuity could occur (cf. discussion in previous paragraphs). For comparison, numerical solutions are shown in figures 1, 2, and 3 for a buoyancy flux varying with time according to (2.11) with values of $p = 1$, 2 and 10 respectively.

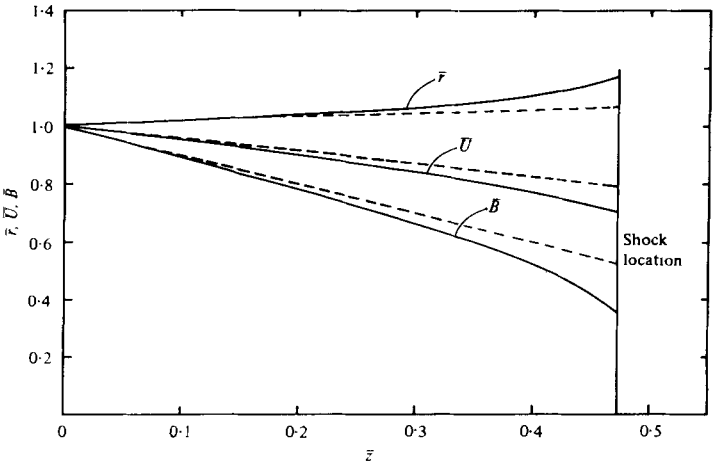

FIGURE 2. Legend as figure 1, but $p = 2{\cdot}0$.

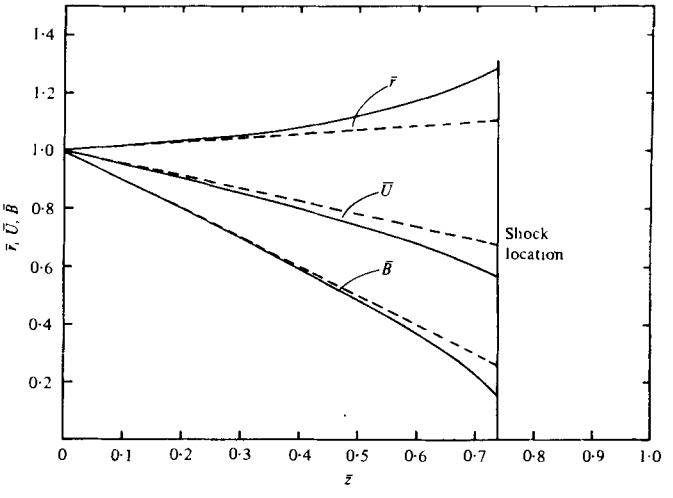

FIGURE 3. Legend as figure 1, but $p = 10{\cdot}0$.

Together with the numerical solution, a first-order analytical approximation is plotted. The asymptotic solution has been found by simple asymptotic analysis of the normalized equations (3.4) and has the form (for small $\bar{z}$):

$$\bar{r} = 1 + \frac{2(\lambda^2+2)}{49}\bar{z}, \tag{3.8a}$$

$$\bar{U} = 1 - \frac{13(\lambda^2+2)}{98}\bar{z}, \tag{3.8b}$$

$$\bar{B} = 1 - \frac{44\lambda^2+34}{38}\bar{z}. \tag{3.8c}$$

It is important to note that the asymptotic solution is independent of the power law dependence (p) and is very close to the numerical solution, for almost all values of $\bar{z}$ (see figures 1, 2 and 3). This means that the normalized properties of the plume expressed as a function of the independent variable $\bar{z}$ are essentially independent of the

exact value of the exponent p, equation (2.11). It can be shown that the independent variable $\bar{z}$, in terms of physical variables, is equal to

$$\bar{z} = \frac{1}{F(t)} \frac{dF(t)}{dt} \frac{z}{U_0(z,t)}, \tag{3.9}$$

where $F(t)$ is the buoyancy flux [(2.11)], and $U_0(z)$ is the quasi-steady axial plume velocity at height z with a buoyancy flux $F(t)$ at the origin. Equation (3.9) shows that the independent variable $\bar{z}$ is essentially the ratio of the flow time $[z/U_0(z,t)]$ versus a time characteristic of the unsteadiness of the buoyancy flux at the source $F/(dF/dt)$.

4. Comparison with experimental results

There are no reported experiments with unsteady buoyant plumes. However, there is extensive literature on temperature profiles in plumes generated from fires, especially near the ceiling over the fire source. For steady or nearly steady (quasi-steady) fires, the temperature excess near the ceiling over the fire source has been correlated (see, e.g. Heskestad 1972) by

$$\frac{\Delta T_0}{Q^{\frac{2}{3}} H^{-\frac{5}{3}}} = 0{\cdot}17 \text{ to } 0{\cdot}23 \,^{\circ}\text{C m}^{\frac{5}{3}}/\text{W}^{\frac{2}{3}}, \tag{4.1}$$

where ΔT_0 is the temperature excess in °C, Q is the heat release rate (assuming complete combustion) in watts, and H is the distance from the top of the fuel to the ceiling in metres. Equation (4.1) has been found experimentally (Yokoi 1960) to hold for the axial temperature excess above the fire, with axial distances (H) measured from the top of the fuel two to three times the horizontal scale of the fire source. However, the constant value of the ratio at the left-hand side of (4.1) has been observed to vary (from a value of 0·17 to 0·23) in independent experimental investigations (Yokoi 1960) with different fuels. Putting aside experimental uncertainties, this discrepancy may be accounted for by two observations:

(i) The heat release rate, Q, in (4.1) should be replaced by the convective component of heat release only, denoted by Q_c. In general, Q includes both the convective and the radiative heat flux generated by the fire. It is known that in turbulent fires (see, e.g. Markstein 1976) the convective heat release rate is a fraction of the theoretical heat release rate; the fraction varies with the fuel. The convective heat release rate has the following relation (Heskestad 1972) to an equivalent buoyancy flux:

$$F = \frac{Q_c g}{\rho_0 C_p T_0}, \tag{4.2}$$

where C_p is the specific heat of the gases and ρ_0 and T_0 are the density and the absolute temperature of the ambient air. It is noted that (4.1) is similar to the temperature excess (or density deficiency) equation reported in steady plumes with a virtual source located on top of the fuel.

(ii) Although a virtual source location on top of the fuel is consistent with limited experimental evidence, relatively small displacement of the virtual source may have a significant effect on the value at the right-hand side of (4.1), expecially for small distances above the top of the fuel source.

Notwithstanding the above objections, (4.1) has proven to be a very useful tool in calculating the temperature over a steady or quasi-steady fire. However, in developing

fires (4.1) does not hold true (Heskestad 1972). Specifically, in the initial period after ignition the left-hand side of (4.1) takes on increasing values with time, but remains less than the quasi-steady value, while well into the fire it takes on a constant value (quasi-steady conditions) in the range specified by (4.1). These observations were a motivation for the present work.

Experimental results of the temperature excess near the ceiling over the fire centre for unsteady fires (generating unsteady buoyant plumes) are now presented in terms of the variables deduced from the theoretical analysis. It should be emphasized that the temperature excess at a point (in the present case a point near the ceiling over the fire centre) depends on the position of the point relative to the thermal and plume behind the thermal. However, in all the fires analysed the thermal cap (transformed to a ceiling jet) has passed the area above the fire before an appreciable temperature excess was reported. Therefore, the solutions derived in §3 (valid inside the plume) can be justifiably used to correlate the experimental results.

Experimental results from tests conducted in two different programs were analysed: (i) Two fire tests (no. 41 and no. 35) (Delichatsios 1976*a*) of 4·6 m high plastic storage fires with 13·7 m ceiling clearance were selected because the fuel was homogeneous and, hence, there was no ambiguity in calculating the heat release rate. (ii) Two fire tests were selected (Heskestad & Delichatsios 1977), wherein wood cribs ignited at the centre of their bases were the fire source. Such wood crib configurations provide reproducible growing fires (Delichatsios 1976*b*) with heat release rate increasing with the second power of time.

The experimental results are plotted in figure 4. In this figure the ordinate is the ratio of the instantaneous measured value of the temperature excess near the ceiling over the fire centre to the corresponding 'quasi-steady' value ($\Delta T/\Delta T_0$). The abscissa is essentially the dimensionless variable $\bar{z}$ [cf. (3.9)].

The ordinate was deduced from the data in the following manner. The ratio defined by the left-hand side of (4.1) was calculated from the raw data at various times after ignition (ΔT_0) was measured by a sensitive thermocouple; Q was calculated from the product of the burning rate (deduced from weight loss measurements) and the measured heat of combustion; finally, H was taken constant and equal to the distance from the top of the fuel to the ceiling [cf. discussion after (4.1)]. The ratio in the left-hand side of (4.1) assumed a constant value (in the range 15 to 21) for times well into the fire development; this value was assumed to be the so-called quasi-steady [cf. (4.1)] value. Finally, the ordinate was determined by dividing the value of the left-hand side of (4.1) at various times over its 'quasi-steady' value, as previously determined.

The abscissa, $\bar{z}$, was calculated by means of (3.9), wherein the quasi-steady value of the velocity, U_0, has been estimated from the equation (Heskestad 1972):

$$\frac{U_0}{Q^{\frac{1}{3}}H^{-\frac{1}{3}}} = 0{\cdot}089 \text{ to } 0{\cdot}092\,\mathrm{m}^{\frac{4}{3}}/\mathrm{W}^{\frac{1}{3}}\,\mathrm{s}, \tag{4.3}$$

and the vertical distance was taken equal to H, the distance from the top of the fuel to the ceiling. In (4.3), Q is expressed in watts, H in metres and Φ_0 in metres per second. It follows that the dimensionless co-ordinate in figure 4 is given by

$$\bar{z} = \frac{1}{0{\cdot}09}\left(\frac{H^4}{Q}\right)^{\frac{1}{3}}\frac{p}{t} = \frac{1}{0{\cdot}09}\left(\frac{H^4}{Q}\right)^{\frac{1}{3}}\frac{1}{Q}\frac{dQ}{dt}, \tag{4.4}$$

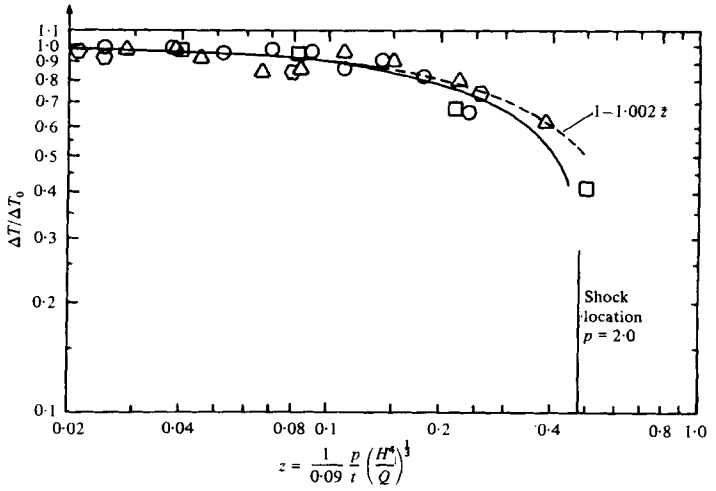

FIGURE 4. Comparison of experimental results with the theoretical predictions: temperature histories over ignition expressed as fractions of the quasi-steady values versus time expressed in terms of the dimensionless parameter $\bar{z}$. Early times correspond to large values of $\bar{z}$. (t in s, H in m, Q in W.) ——, numerical solution for $p = 2{\cdot}0$; – – –, asymptotic solution (independent of p); $\lambda = 1{\cdot}16$.

H (effective height) in m	p
○, 7·90	2·0
△, 8·50	2·0
□, 13·7	11·0
⬡, 13·7	1·0

with the height H in metres; Q in watts; the time in seconds, and an assumed constant in (4.3) equal to 0·09. The power exponent approximating the fire behaviour and the height from the top of the fuel to the ceiling are listed in figure 4 for each of the fire tests.

The asymptotic solution (which is independent of p), together with the numerical solution for $p = 2{\cdot}0$ is included in figure 4. The agreement with the experimental results is remarkable. Ih addition, it is to be noted that the temperature history, expressed in terms of the normalized variables in figure 4, is essentially independent of the power exponent p, (2.11); this behaviour is consistent with the theoretical predictions included in the discussion at the end of § 3 [cf. (3.8)].

5. Conclusions

There are four major results of the present work:

1. A time similarity formulation of the unsteady plume equations has been developed;

2. A similarity formulation is possible only if the buoyancy flux is a power law function of time;

3. The velocity of the base of the thermal (leading edge of the plume) preceding the plume is shown to be less than the 0·42 fraction of the velocity inside the plume at the same level;

4. Numerical and asymptotic solutions of the unsteady plume equations have been favourably compared with experimental temperature histories over growing fires. Both

the theoretical and the experimental results indicate that temperature histories expressed in terms of the normalized variables, shown in figure 4, are only slightly dependent on the power exponent appearing in the power law dependence on time of the buoyancy flux.

REFERENCES

DELICHATSIOS, M. A. 1976*a* Fire growth rates and sprinkler response in small-scale stored plastics tests. *FMRC Tech. Rep.* no. 22503, Factory Mutual Research Corporation, Norwood, Massachusetts.

DELICHATSIOS, M. A. 1976*b* Fire growth in wood cribs. *Combustion and Flame* **27**, 267.

HANSEN, A. G. 1967 *Generalized Similarity Analysis of Partial Differential Equations in Nonlinear Partial Differential Equations* (ed. W. F. Ames), p. 1. Academic Press.

HESKESTAD, G. 1972 Similarity relations for the initial convective flow generated by fire. *A.S.M.E. paper no.* 72-WA/HY-17.

HESKESTAD, G. & DELICHATSIOS, M. A. 1977 Environments of fire detectors. Phase I: Effect of fire size, ceiling height and material, vol. 1, Tests; vol. 2, Analysis. *F.M.R.C. Tech. Rep.* no. 22427, Factory Mutual Research Corporation, Norwood, Massachusetts.

MARKSTEIN, G. H. 1976 Radiative energy transfer from turbulent diffusion flames. *Combustion and Flame*, **27**, 51.

MIDDLETON, J. H. 1975 The asymptotic behaviour of a starting plume. *J. Fluid Mech.* **72**, 753.

MORTON, B. R. 1959 Forced plumes. *J. Fluid Mech.* **5**, 151.

TURNER, J. S. 1962 The starting plume in neutral surroundings. *J. Fluid Mech.* **13**, 356.

WITHAM, G. B. 1965 Nonlinear dispersive waves. *Proc. Roy. Soc.* A **283**, 238.

YOKOI, S. 1960 *Report of the Building Research Institute*, no. 34, Ministry of Construction, Japan.